Local structural variability and the intermediate phase window in network glasses

A. Sartbaeva, S. A. Wells, A. Huerta,* and M. F. Thorpe
Department of Physics and Astronomy, Arizona State University, Tempe, Arizona 85287-1504, USA
(Received 25 October 2006; revised manuscript received 9 January 2007; published 14 June 2007)

Recent experimental work has shown that the width of the intermediate phase varies considerably in chalcogenide glasses containing Ge/As/Se. As the chemical composition is varied within a series of glasses, three phases are observed. As the mean coordination of the glass is increased, the floppy phase evolves through the intermediate phase (rigid but unstressed) into the rigid and stressed phase. Here, using an extensive study of computer-generated networks, we show that the intermediate phase is caused by self-organization. This is only possible on networks where the single transition, from the floppy to the rigid and stressed phase, is second order in the absence of self-organization, which leads the network to be responsive to self-organization. This occurs when the structural variability—a measure of inhomogeneities within the glasses—exceeds a threshold value. The width of the intermediate phase is associated with the local structural variability. Above the threshold value, a large structural variability leads to a wider intermediate phase, which we refer to as the intermediate phase window.

DOI: 10.1103/PhysRevB.75.224204 PACS number(s): 61.43.Fs, 05.65.+b, 61.43.Bn, 64.70.Pf

I. INTRODUCTION

The theoretical prediction[1] and experimental discovery[2] of the intermediate phase have opened up a new window on glasses, both in terms of the fundamental properties of covalent networks,[3–5] and also on potential applications.[2,6–14] The *intermediate phase* is a range of compositions for which the glass transition acquires a thermally reversing character,[12] that is, the nonreversing enthalpy of the glass transition goes to zero. The intermediate phase exists as a function of the chemical composition and so is very demanding to study experimentally as each data point requires a separate sample.

In chalcogenide glasses such as Ge_xSe_{1-x}, it is convenient to describe the transition by the mean coordination $\langle r\rangle$, which in this case is given by $\langle r\rangle = 4x + 2(1-x) = 2 + 2x$, where the Ge ion is fourfold coordinated and the Se ion is twofold coordinated. In simulations of the rigidity of glassy networks,[1] three phases can be observed as $\langle r\rangle$ is increased: an initial "floppy" phase without percolating rigidity, a "rigid" phase in which a rigid cluster percolates across the network, and a "stressed" phase in which portions of the rigid structure become overconstrained. A "rigid cluster" is a portion of the system with an exact balance of the degrees of freedom and constraints, while a "stressed region" has more constraints than degrees of freedom. The rigid phase is observed, over a narrow range of values of the mean coordination $\langle r\rangle$, only when the network is *self-organized*. By self-organization, we mean that the network avoids creating overconstrained, stressed regions unless there is no alternative. In this case, self-organization involved starting with the floppy phase at low mean coordination, and then increasing the mean coordination by adding bonds, in such a way as to avoid stress for as long as possible.[15] This leads us to identify the experimental intermediate phase with the rigid phase. Without any self-organization,[1] there is a single transition from floppy to rigid and stressed (without any intermediate phase) that occurs at close to a mean coordination $\langle r\rangle = 2.4$, which corresponds to a chemical composition $x = 0.2$ and $GeSe_4$. For more complex glass series such as $Ge_xAs_ySe_{1-x-y}$, the intermediate phase also occurs around a mean coordination of $\langle r\rangle = 2.4$, which corresponds[14] to $2.4 = 4x + 3y + 2(1-x-y) = 2 + 2x + y$. We argued that the appearance of the intermediate phase was linked to self-organization in glasses in a quite general way.

Barré *et al.*[16] have considered a thermodynamically proper model with an energy cost associated with stress and showed that in the canonical ensemble, the intermediate phase still exists. In recent papers, Brière *et al.*[17] and Chubynsky *et al.*[18] confirmed this result for the $T=0$ version of the model of Barré *et al.*, and also have shown that the intermediate phase is entropically feasible in actual physical systems. In both the models of Barré *et al.* and Chubynsky *et al.*, the intermediate phase has an unusual property: both nonpercolating and percolating networks coexist in the ensemble at all mean coordination numbers within the intermediate phase. Micoulaut[19] has pointed out the significance of local structure selection (speciation) in the development of the intermediate phase. In a careful study on the nature of the intermediate phase, Brière *et al.*[17] have shown that the system remains *critical* throughout the intermediate phase. This means that at any point in the intermediate (rigid) phase, the addition of a single constraint without self-organization can make the system overconstrained (stressed). This provides a fascinating new insight.

The phase transition from floppy to rigid occurs when the number of constraints exactly equals the number of degrees of freedom. When this condition exactly holds, the system is said to be isostatic. In the absence of self-organization, this occurs at a single point when the mean coordination $\langle r\rangle$ is 2.4. However, with self-organization, we can maintain the infinite percolating rigid cluster in the isostatic state over a range of values of $\langle r\rangle$ by using the self-organization to increase the number of sites in the infinite cluster, until the whole system is isostatic. This is accomplished by filling in the regions between the dendrites in the infinite cluster, thus increasing its effective fractal dimensionality from below 3 at the flexible phase to intermediate phase transition to 3 at the intermediate phase to stressed phase transition.

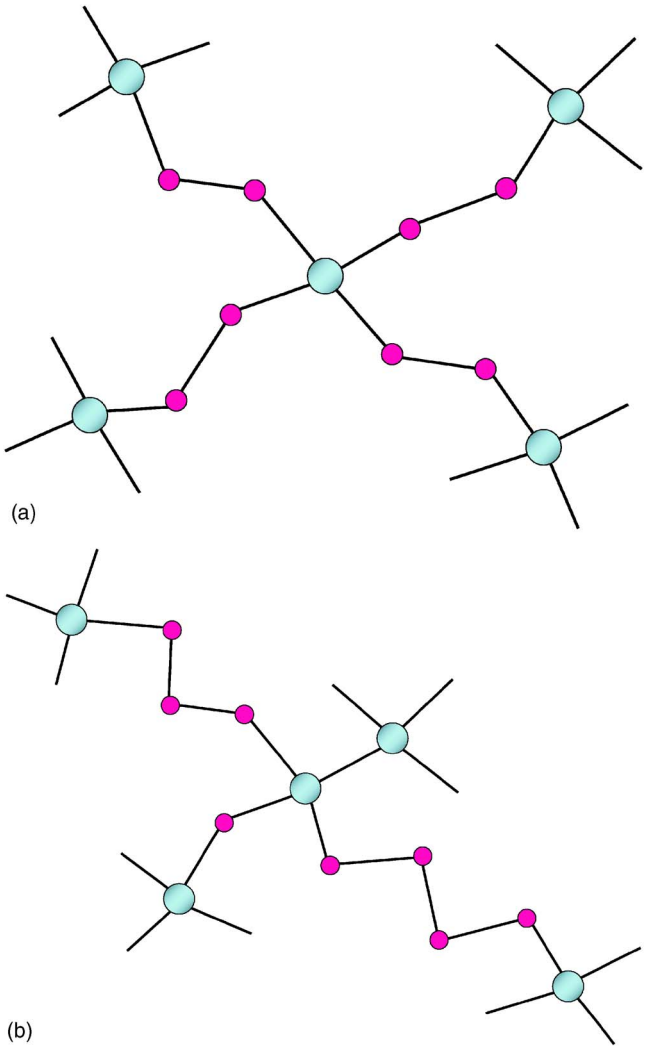

FIG. 1. (Color online) Two possible variations of the Se chain lengths for the composition $GeSe_4$. Light blue, (four-coordinated) Ge atoms; pink, (twofold coordinated) Se atoms. (a) Se chain lengths all equal 2. (b) Se chain lengths ranging in length between 0 and 4.

In this paper, we take these ideas further by studying the actual width of the intermediate phase as determined by the self-organization of various kinds of network, and also the nature of the two distinct phase transitions from floppy to intermediate and from intermediate to stressed rigid. We find that the determining factor is the structural variability v or local (i.e., atomic level) inhomogeneity within the glass. We define v in terms of constraints later; for now a qualitative example will suffice. If $GeSe_4$ glass showed no local structural variability, then each pair of neighboring Ge atoms would be bridged by a chain consisting of exactly two Se atoms. In practice, Ge sites can be connected by a homopolar (Ge-Ge) bond, by chains of variable length, or by a shared tetrahedral edge (Fig. 1); this variation in bonding patterns is what we mean by structural variability.

For self-organized systems with *small* structural variability, we find no intermediate phase. As a threshold value of the structural variability v is passed, the width of the intermediate phase increases from zero. The upper phase transition from intermediate to rigid is found to be pinned at a mean coordination of $\langle r \rangle = 2.4$ and to be always first order for any value of v. The key to understanding this behavior is the magnitude of the structural variability in the network without self-organization. If the structural variability is below the threshold value, the single transition is first order and there is no intermediate phase when self-organization is introduced. On the other hand, if the structural variability is above this threshold value, the phase transition is second order, and self-organization produces an intermediate phase, whose width increases with the magnitude of the structural variability. We refer to this as the *intermediate phase window*.

Our approach to introducing self-organization and structural variance is described in Sec. II. In Sec. III, we describe our results for non-self-organized (III A) and for self-organized (III B) networks. In Sec. IV, we look at the implications of these results for real glasses and try to interpret the observed widths of the intermediate phase in terms of the structural variance v.

II. METHOD

We model the Ge/Se glass system starting with a three-dimensional model of four-coordinated atoms in an amorphous, glassy network. We use this as a model for the topology of links between Ge atoms. We took glassy models from Ref. 20 containing 216, 512, and 4096 Ge atoms. From these models, we created supercells so as to have networks with periodic boundary conditions containing different numbers of atoms. From the 216 atom model, we created supercells with 1728, 5832, 13 824, 27 000, and 46 656 Ge atoms; from the 512 atom model, we created supercells with 512, 4096, 13 824, 32 768, and 64 000 Ge atoms; and from the 4096 model, we created 4096 and 32 768 Ge atoms.

Each Ge-Ge link is then decorated with a chain of Se atoms of length l. The value of l is chosen for each Ge-Ge link from a user-defined probability distribution, for example, a roughly flat distribution between a minimum and a maximum length. We used a variety of different distributions when decorating the networks, so that the initial nominal composition of networks varied from $GeSe_{2.5}$ to $GeSe_5$. The rigidity transition always happens near the composition of $GeSe_4$. In Fig. 1, we show two examples of decoration, one with uniform chain lengths and one with variable chain lengths. This decoration is purely topological, and the rigidity analysis depends *only* on the constraints defined by the bonds between atoms and not on the exact atomic positions. In this decoration, we do not introduce edge-sharing tetrahedra; however, the effect of this structural motif can be introduced by a renormalization argument, as discussed later in Sec. IV.

The rigidity analysis is carried out using the PEBBLE GAME (Refs. 21 and 22) implemented in FIRST (Ref. 7) and a body-bar representation of the network.[23] In this representation, an atom is an orientable rigid body with six degrees of freedom (DOFs). Bonds between atoms are considered as "bars" where each bar removes one DOF from the system. We keep bond lengths and angles fixed, while dihedral angles are *a priori* variable. In general, a rotatable bond between two at-

oms is represented by five bars, as is clear from the following argument. Initially, we have two atoms each with six DOFs; by introducing a rotatable bond between them, we produce a two-atom body (with six rigid-body DOFs) with one internal degree of freedom (rotation about the bond), giving a total of seven DOFs. The bond has thus removed five DOFs from the system. The importance of $\langle r\rangle = 2.4$ is now clear; if each atom in the system has 2.4 bonds on average, then the system contains an average of $(2.4\times 5)/2 = 6$ constraints per atom.

For computational efficiency, we have performed the rigidity analysis with only the fourfold (Ge) atoms present, which we refer to as "nodal" atoms. The twofold coordinated (Se) atoms are not represented explicitly; instead, each chain of Se atoms is renormalized to give an effective number of constraints between the two Ge atoms at the ends of the Se chain. This renormalization proceeds as follows. Consider two Ge atoms covalently bonded together; the bond between them is represented as five bars. We can consider this as a chain of length zero (no Se atoms between the Ge atoms). If we now introduce one Se atom between the Ge atoms, making a chain of length 1, then we have removed a Ge-Ge bond (five bars) and added a Se atom (six degrees of freedom), so the system gains $5+6=11$ DOFs, and we have added two new rotatable bonds (Ge-Se-Ge), so the system loses $5+5=10$ DOFs. The effect of increasing the chain length by 1 was thus to increase the DOF of the system by $11-10=1$. We can thus represent the connection of two Ge atoms by a chain of length 1 as a Ge-Ge bond with four bars instead of five. In general, a chain of l Se atoms is represented as a Ge-Ge bond with $(5-l)$ bars when l is less than 5. When l is greater than or equal to 5, then the constraint between the Ge atoms is effectively absent (from a rigidity viewpoint) as the number of bars has dropped to zero. In the rigidity analysis, it is as if there were no Ge-Ge connection at all when the Se chain length is 5 or higher.

We must also renormalize the counting of the mean coordination of the system to reflect our treatment of the chains. When a Se chain has length 4 or less, then the Se atoms in that chain are considered *present* in the system and are counted as two-coordinated atoms. If, however, a chain has length equal to 5 or greater, then the count changes. Firstly, the Se atoms in the chain are effectively not present in the system for rigidity purposes, so they do not count toward either the total number of atoms or the number of twofold atoms. Secondly, the coordination of the Ge atoms at the ends of the chain is reduced by 1; for example, if two Ge atoms are each connected to three chains of length 4 or less, but they are linked together by a chain of length 5 or greater, then those two Ge atoms count not as fourfold coordinated but as threefold, since the chain between them is absent in the rigidity analysis.

If all chain lengths in the system are 4 or less, then this renormalization has no effect on the count and the mean coordination will be the same as that calculated based only on the chemical composition. If, however, any chain length is 5 or greater, then the renormalized mean coordination will differ from the chemical mean coordination. The discussions of mean coordination below refer to the renormalized form. In practice, we find that the effect of this renormalization is very small and is outweighed by the effect of other structural motifs such as edge sharing, as discussed below.

We wish to observe the variation of the rigidity of the system as its composition varies. We start with a defined topology of Ge-Ge connections and decorate it with Se chains of variable length (note that if the average chain length is $\langle l\rangle$, then the chemical formula of the system will be $GeSe_{2\langle l\rangle}$). We perform a rigidity analysis on the system using the PEBBLE GAME; this step is fast even for the large systems used here. We then vary the composition by selecting a candidate Se atom to remove. This selection can be made either by choosing any Se atom with equal probability or by choosing any chain with equal probability and then removing an atom from that chain. The principal difference between the two approaches is that selection by atom tends to remove atoms from the longer chains preferentially and thus reduces the variability of chain lengths. It proved essential to use selection by chain to produce large variability. A trial move is to eliminate the chosen Se atom from the system (reducing the length of that chain by 1) and recalculate the rigidity of the system.

Each time the rigidity of the system is checked, we obtain information on the size of the largest rigid cluster (group of mutually rigid Ge atoms) and the largest stressed cluster. We also perform a percolation test to determine whether the largest rigid cluster has percolated across the cell or not. This test requires that the largest rigid cluster spans the cell in *all three* Cartesian directions. The removal of Se atoms from the system can be performed in either a completely random or a self-organized fashion. If the removals are completely random, then every trial move is accepted. If, on the other hand, we enforce self-organization, then trial moves are rejected if they would create a stressed region in the system. If a move is rejected, then the Se atom is removed from the list of candidates, as are all Se atoms in the same chain, as we now know that shortening that chain will cause stress in the system. Eventually, the list of candidates becomes empty when all atoms that can be removed without causing stress have been removed. At this stage, we must allow moves that cause stress, and the transition from the intermediate phase to the rigid and stressed phase occurs precisely at $\langle r\rangle = 2.4$, as there are no redundant constraints.

We tried a number of parameters associated with the structure in order to better understand and characterize the nature of the phase transitions and, in particular, the width of the intermediate phase. We first define the number of constraints associated with each nodal site, which are the Ge atoms. As noted previously, there are $5-l$ constraints associated with each Se bridge with l atoms, as long as $l \leqslant 5$, otherwise 0. These are summed over the four neighbors of the nodal atom (and divided by 2 as each Se bridge is shared by two nodal Ge atoms) to give the number of constraints associated with each nodal atom i which we will call v_i. The variability v in the number of constraints per nodal Ge atom is then given by

$$v^2 = \frac{1}{N}\sum_{i=1}^{N} v_i^2 - \left(\frac{1}{N}\sum_{i=1}^{N} v_i\right)^2. \qquad (1)$$

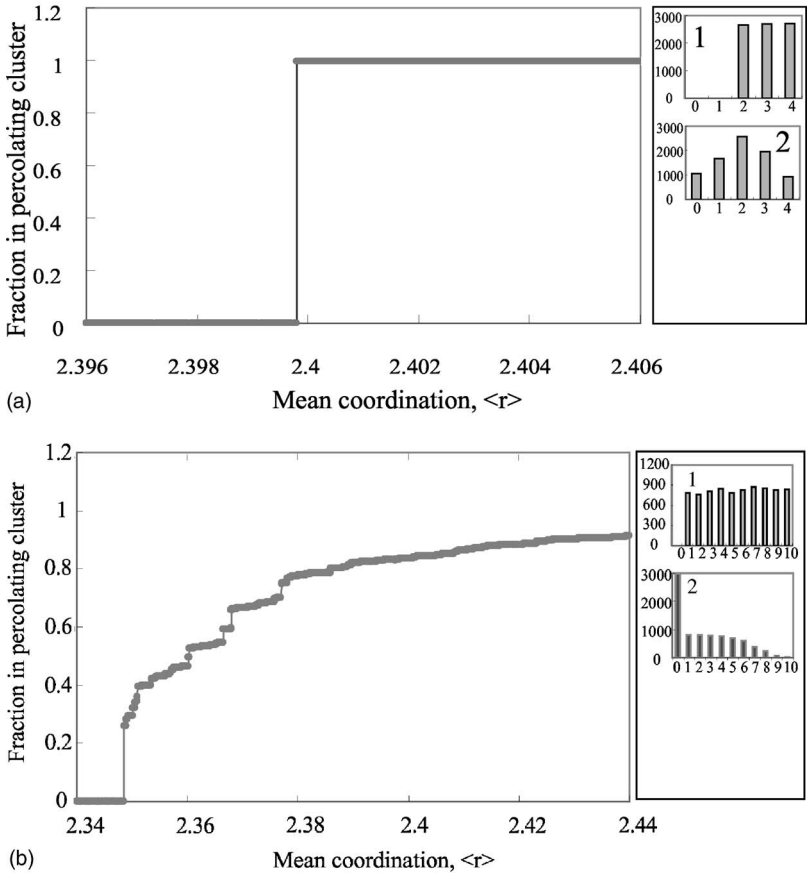

FIG. 2. Fraction of sites in the percolating rigid cluster plotted against mean coordination number $\langle r \rangle$ for a network with 4096 Ge atoms. (a) Se chain lengths, in the initial distribution in the floppy phase, are between 2 and 4, shown in inset 1. Inset 2 shows the distribution of Se chains at the rigidity percolation transition, where structural variability $v=1.19$. (b) Se chain lengths, in the initial distribution in the floppy phase, between 1 and 10, as shown in inset 1. Inset 2 shows the distribution of Se chains at the rigidity percolation transition, where structural variability $v=2.05$.

During the process of removing Se atoms from the system, we track the mean coordination, the structural variability v, and the fraction of Ge atoms in the percolating rigid cluster. For the self-organized case, we also monitor the fraction of Ge atoms in the stressed cluster once stress begins to be created. Self-organization allows for the formation of a *window* between the onset and percolation of rigidity and the onset of stress. When percolation of rigidity or stress occurs, the fraction of atoms in the percolating cluster goes from 0 to a nonzero value; we will refer to this change from zero as a *jump*. The behavior of the jump as a function of system size indicates whether the rigidity transition is first order (jump tends to a nonzero value as system size increases) or second order (jump tends to zero as system size increases).

III. RESULTS

A. Network properties

We begin by carrying out random (non-self-organized) elimination of Se atoms from the system.

In Fig. 2, we present the results for two systems with different initial variations in Se chain lengths. In the first case, we performed chain dilution on a 4096 Ge atom network with a roughly flat distribution of chain lengths between 2 and 4 [Fig. 2(a)], as shown in inset 1. The rigid cluster percolates very close to a mean coordination number $\langle r \rangle = 2.4$. This occurs because here there are no redundant bonds, by construction, and so the Maxwell count is exact. When rigidity percolates, the fraction of Ge atoms in the percolating rigid cluster jumps to almost 1 [Fig. 2(a)] in a first-order transition. In inset 2 [Fig. 2(a)], we show the distribution of Se chains at the rigidity percolation transition. It is interesting to note that even though in the initial system we did not introduce any chains of length zero (corresponding to a Ge-Ge bond), in the subsequent distribution, some homopolar bonds do appear. Also, despite starting from a roughly flat distribution, the system adopted a peaked distribution with an average around 2.

In the second case with a larger variability in chain lengths [Fig. 2(b)], we see a totally different picture. We started with a roughly flat distribution of Se chain lengths between 1 and 10, as shown in inset 1, Fig. 2(b). At the rigidity percolation transition, the system has developed a large amount of homopolar Ge bonds ($l=0$) and the distribution is decaying with a long tail, i.e., there are still some long chains present [Fig. 2(b), inset 2]. The prominent feature in this case is that the jump decreases and the transition becomes more second-order like. We noticed a strong dependence of the jump on the size of the system, when the variability is large. In this case, the larger the system, the smaller the size of the jump (for example, for the system with 4096 Ge atoms, the average jump=0.5; for the system with 32 768 Ge atoms, the average jump=0.23; and for the system with 64 000 Ge atoms, the average jump=0.11). Figure 3 shows the jump against inverse system size (where N is the number of Ge atoms). Clearly for an initial chain distribution with lengths from 2 to 4, the transition is first order in the limit of infinite system size. On the other hand, for chain lengths initially from 1 to 10, the jump tends to zero in the limit, and

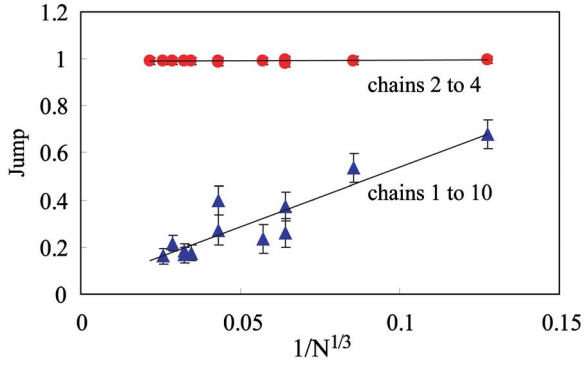

FIG. 3. (Color online) Jump in the fraction of Ge atoms in the percolating cluster plotted against the inverse linear system size, $1/N^{1/3}$, where N is the number of Ge atoms, for the initial chain distribution with lengths from 2 to 4 (circles) and from 1 to 10 (triangles). See the upper right insets 1 in Figs. 2(a) and 2(b). Systems with initial chain lengths 2–4 extrapolate to 1 in the limit of infinite N, while systems with initial chain lengths 1–10 extrapolate to zero.

the transition from floppy to rigid is second order.

In both of these cases, percolation of stress (not shown) occurs immediately after percolation of rigidity. In the absence of self-organization, there is no intermediate phase, of course.

By setting up systems with different initial distributions of chain lengths, we can observe the rigidity transition taking place at different values of structural variability. In Fig. 4, we show the jump at the rigidity transition extrapolated to the large N limit. At low structural variabilities (less than 1.5), the transition is clearly first order, while at high structural variabilities (above 1.7), it is clearly second order. In the region of the change between first- and second-order behaviors, it is difficult to extract the precise infinite-size limit due to large fluctuations; note the large error bars on this portion of the graph. However, it would seem that there is a tricritical point around $v=1.55$.

The variability in the Se chain lengths, which leads to the structural variability, appears to be the parameter that controls the width of the intermediate phase window. We have also checked the skewness and kurtosis [Figs. 5(a) and 5(b)],

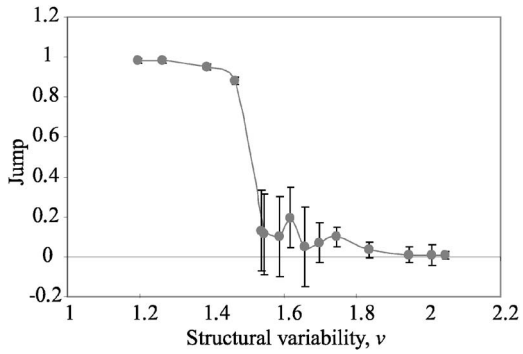

FIG. 4. Jump in the fraction of Ge atoms at the transition in the percolating cluster plotted against the structural variability in the number of constraints per nodal Ge site for non-self-organized networks.

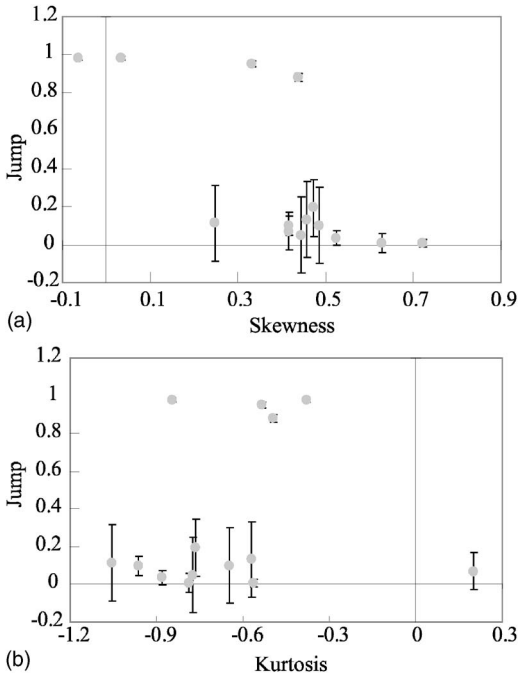

FIG. 5. Jump in the fraction of Ge atoms in the percolating cluster versus (a) skewness and (b) kurtosis for non-self-organized networks, showing no clear correlation.

as possible alternative parameters, but there appears to be no correlation between those parameters and the jump of the percolating rigid cluster.

B. Self-organized networks

In Fig. 6, we present the results for two systems with different initial variations in Se chain lengths, as before. This time, however, we eliminate Se atoms using self-organization, that is, rejecting choices that would introduce stress into the system, until it becomes inevitable. We present results on the percolation of the rigid and stressed clusters separately, as they are now distinguishable by different percolation thresholds.

In the first case, we performed chain dilution on a 4096 Ge atom network with an initial roughly flat distribution of chain lengths from 2 to 4 [Fig. 6(a)], as shown in inset 1. Both rigid and stressed clusters percolate very close to a mean coordination number $\langle r\rangle=2.4$. When rigidity percolates, the fraction of Ge atoms in the percolating rigid cluster jumps to almost 1 [Fig. 6(a)] in a first-order transition. Stress percolation is similarly first order, and there is no intermediate phase. In inset 2 [Fig. 6(a)], we show the distribution of Se chains at the rigidity percolation transition and in inset 3 the distribution of Se chains at the stress percolation transition. These distributions appear identical to that for rigidity percolation in the non-self-organized case [Fig. 2(a)]. The small difference in the locations of the two jumps in Fig. 6(a) does not signify an intermediate phase, as the difference only involves a very small, $O(1)$, number of Se atoms and so would be insignificant in the limit of infinite size.

In the second case with a larger variability in chain lengths [Fig. 6(b)], we see a very different picture. We

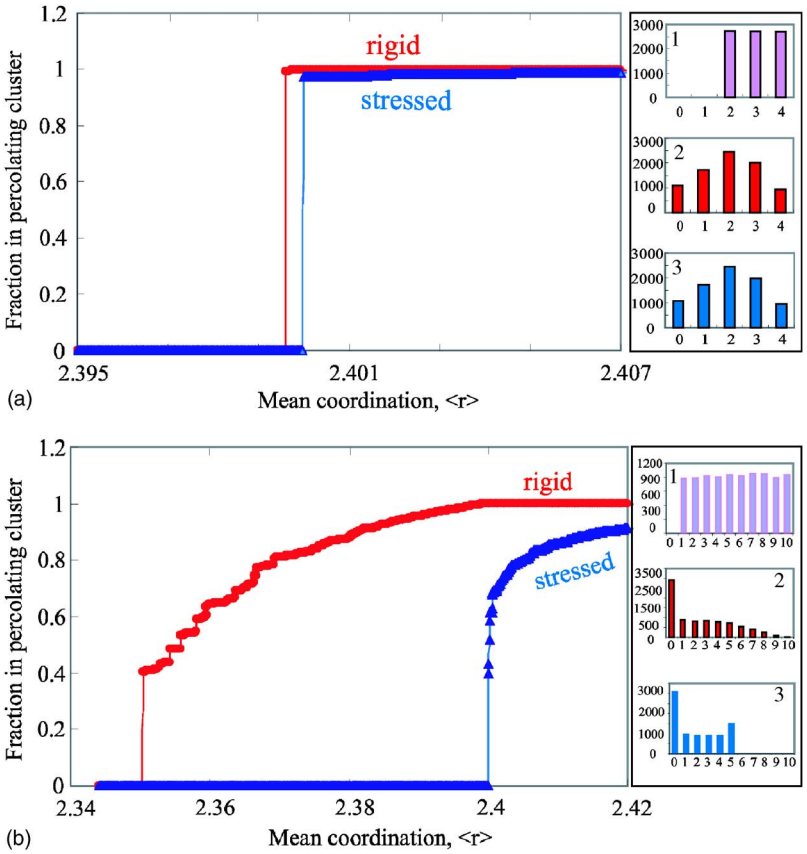

FIG. 6. (Color online) Fraction of sites in the rigid and stressed percolating clusters plotted against the coordination number $\langle r \rangle$ for network with 4096 Ge atoms. (a) Se chain lengths, in the initial distribution in the floppy phase, are between 2 and 4, shown in inset 1. Inset 2 shows the distribution of Se chains at the rigidity percolation transition, where structural variability $v = 1.19$. Inset 3 shows the distribution of Se chains at the stress percolation transition. There is no intermediate phase here. (b) Se chain lengths, in the initial distribution in the floppy phase, between 1 and 10. Inset 1 shows the initial distribution of Se chains. Inset 2 shows the distribution of Se chains at the rigidity percolation transition, where structural variability $v = 2.05$. Inset 3 shows the distribution of Se chains at the stress percolation transition. The intermediate phase window, which is rigid but unstressed, exists for $2.35 < \langle r \rangle < 2.4$.

started with a roughly flat distribution of Se chain lengths between 1 and 10, as shown in inset 1, Fig. 6(b). At the rigidity percolation transition, the system has developed a large amount of homopolar bonds ($l=0$) and the distribution is decaying with a long tail, i.e., there are still some long chains present [Fig. 6(b), inset 2], as in the non-self-organized case shown in Fig. 2. The jump at the rigidity percolation transition is smaller than 1 and the transition appears more second order. At the stress percolation transition, the system has lost all chains longer than 5. This indicates that those long chains were a "reservoir" of flexibility, which allowed the system to have an intermediate phase. Rigidity percolation takes place at $\langle r \rangle \simeq 2.35$, while stress percolation occurs at the critical value of 2.4 and the intermediate phase window exists in the $2.35 < \langle r \rangle < 2.4$.

For each distribution, we have simulated the systems with different sizes, so as to differentiate between the first- and second-order transitions. In Fig. 7, we show the jump at the rigidity transition for self-organized systems in the limit of infinite system size. At low structural variabilities (less than $\simeq 1.5$), the transition is clearly first order, while at high structural variabilities (above 1.7), it is clearly second order. In the region of the change between first- and second-order behaviors, it is difficult to extract the precise limit due to large fluctuations; note the large error bars on this portion of the graph. However, it would seem that there is a tricritical point around $v = 1.55$, where the character of the transition changes from first order to second order. For $v \leqslant 1.55$, self-organization is irrelevant and cannot produce an intermediate phase. This is because the transition is first order and there are no critical fluctuations. For $v \geqslant 1.55$, self-organization can work with the inherent fluctuations associated with the second-order transition to produce an intermediate phase window. Note the similarity of Figs. 4 and 7.

IV. DISCUSSION

In the self-organized network, there is a window between the percolation of rigidity and the onset of stress (see Fig. 6). The onset of stress always occurs at a mean coordination of 2.4; however, the percolation of rigidity occurs at a lower mean coordination, with the difference between this value

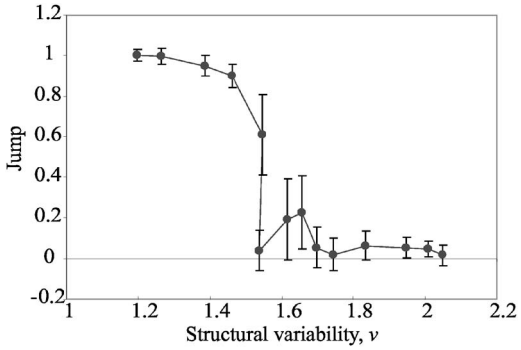

FIG. 7. Jump in the fraction of Ge atoms in the percolating cluster at the lower transition plotted against the structural variability of the number of constraints per nodal Ge site for self-organized network.

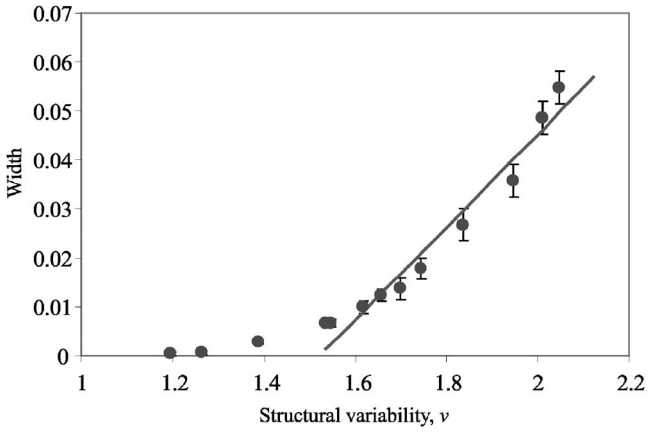

FIG. 8. Width of the intermediate phase window shown against the structural variability v. At low values of the variability, where the transition is first order, the width is zero, within numerical error. At higher variabilities, the width grows roughly linearly with the structural variability, as given by Eq. (2).

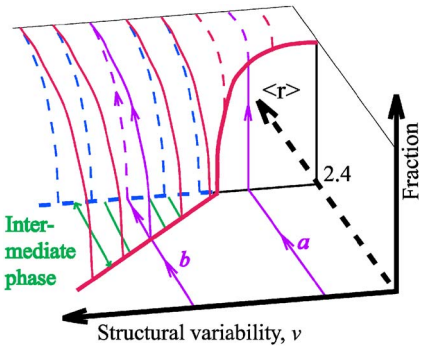

FIG. 9. (Color online) Schematic representation for the phase diagram of glassy networks in terms of structural variability v and mean coordination $\langle r\rangle$. The fraction axis refers to rigid percolating cluster and stressed percolating cluster. The solid line represents second-order transition from floppy to rigid phase. The dashed line represents first-order transition from rigid to stressed phase. Lines a and b represent schematic pathways at different "fixed" structural variabilities.

and 2.4 defining the width of the intermediate phase window (Fig. 8).

In Fig. 8, we plot the width of the intermediate phase window against the structural variability v. At low values of the structural variability, the width is close to zero. At higher structural variabilities, the width grows roughly linearly with the variability. These results are all from extrapolated values in the limit of infinite system size, using the procedure in Fig. 3. The error bars are quite significant although the general trend is clear. Although we cannot say with certainty that the intermediate phase is absent for $v \leqslant 1.55$, we will assume this to be so. The linear fit to the width W through the points in Fig. 5 is given by

$$W = (v - 1.55)/10. \tag{2}$$

This allows us to construct a phase diagram in terms of the structural variability v and coordination number $\langle r\rangle$ shown in Fig. 9. The width of the intermediate phase increases with an increase in structural variability v. This can be easily seen from following lines a and b along the mean coordination $\langle r\rangle$ axis at a "fixed" structural variability v. At low structural variability (line a), the transition happens close to $\langle r\rangle = 2.4$ and has a first-order behavior. There is no intermediate phase and the rigid and stressed phase transitions happen simultaneously. When structural variability is high (line b), there is a gradual second-order transition from floppy to rigid phase and the intermediate phase is present. This is followed by a first-order transition from rigid to stressed phase at $\langle r\rangle = 2.4$.

A. Bonding chemistry

An important question is whether such a degree of variation in the constraints per nodal site is physically reasonable in terms of the bonding chemistry of the GeSe system. This is a difficult question to answer as the bonding in GeSe glasses is not well understood, in terms of the lengths of the Se chains that link pairs of Ge atoms. It does, however, appear that bonding in GeSe systems is quite heterogeneous. NMR data indicate that Se chains of length 1 and length 3 or more are present[24] in roughly equal numbers in $GeSe_6$, although this result is strange as it would seem that there should also be a significant number of Se chains of length 2.

Chains of lengths 1, 2, and 3 only are not sufficient for the structural variability needed to produce a window. Let us consider a network of composition close to $GeSe_4$, with an average chain length of 2; suppose that a fraction $(1-r)$ of chains have length 2, while fractions $r/2$ have length 1 and length 3. A chain of length 1 introduces four constraints to the system, which we count as 2 constraints per chain per atom. A chain of length 2 introduces 3/2 constraints per chain per atom, and a chain of length 3 introduces 1 constraint per chain per atom. The mean number of constraints per chain per atom is $c=3/2$, while the root-mean-square deviation (rmsd) is given by the square root of the quantity $[(r/2)(2-3/2)^2+(1-r)(0)+(r/2)(1-2/3)^2]$, that is, $(\sqrt{r}/2)$. Each atom is connected to four chains, so that if the lengths of the chains are not correlated, the rmsd on the number of constraints per atom—that is, the structural variability v—is just $(\sqrt{4})(\sqrt{r})/2$, which is $\sqrt{r}$. So even in the extreme case where $r=1$, $v=1$, this is not sufficient for a window.

Raman scattering[2] indicates the presence of a wide variety of structural motifs including edge- and corner-sharing GeSe tetrahedra, Se chains of length 2 and greater, direct Ge–Ge bonding, and pseudotetrahedral bonding (Ge–Se with a one-coordinated Se atom); the last, where the Se is terminal rather than bridging, corresponds to 0 bonding constraints as it does not link to another nodal site, in terms of rigidity. Neutron-scattering data on $GeSe_2$ (Refs. 25–27) still indicate considerable breaking of chemical ordering, with up to 25% of Ge and 20% of Se atoms being involved in homopolar bonds rather than a network of corner-sharing GeSe tetrahedra. It therefore does seem quite reasonable that the constraints per nodal site in real GeSe systems can vary considerably, as required to allow a nonzero width of the intermediate phase.

B. Effect of edge-sharing tetrahedra

Probably the most important structural motif, present in the chemistry of the GeSe system but not in our model, is the edge-sharing tetrahedral motif. In this case, two Ge atoms are connected by two chains of length 1. This has an important consequence for rigidity analysis; although in general a chain of length 1 introduces four constraints between Ge atoms, and two such chains introduce eight constraints, the net effect of the edge-sharing motif is to rigidify the two adjacent tetrahedra involved, which corresponds to the removal of only six constraints total. Thus, even though the edge-sharing tetrahedral motif is locally rigid, its effect on the system is (paradoxically) to make the system less constrained than the chemical composition would indicate. This suggests a resolution to a puzzling issue in comparing experimental and theoretical results; in our simulations, the floppy to rigid transition always occurs *below* $\langle r\rangle=2.4$, while the rigid to stressed transition occurs *at* $\langle r\rangle=2.4$. Experimentally, however, the GeSe system displays a window between $\langle r\rangle'=2.4$ and $\langle r\rangle'=2.52$ (Refs. 2 and 3) (according to the chemical composition), that is, the window is displaced to a higher $\langle r\rangle'$ than the theoretically expected position. We may describe the window in terms of a center and a width, noting that the width of the experimental window is larger and the position of the center is higher than our theoretical results.

Although we did not explicitly include any edge-sharing tetrahedral bonding when constructing our model, we can introduce them into our analysis by the following renormalization-type argument. Let us consider a single Ge site with four links to other Ge sites. We can, *without affecting the rigidity of the network*, replace this Ge site by two Ge sites and two Se bridges, representing edge-sharing tetrahedral bonding. Each of the newly introduced Ge takes up a pair of the incoming links; the Ge_2Se_2 cluster is a single rigid body, and so the rigidity of the network is unaffected. Thus, any of our models of a Ge/Se system, in fact, represents a whole series of models with a variable proportion of edge-sharing motifs added.

Let us say that we have a network of composition Ge_xSe_{1-x} containing no edge-sharing motifs, representing one of the networks in our rigidity analysis. We replace a fraction f of Ge sites with Ge_2Se_2 edge-sharing motifs. Each such motif introduces an additional $GeSe_2$ unit into our system, changing the composition to $Ge_{(1+f)x}Se_{2fx+(1-x)}$. The system now has the same rigidity properties and a new composition Ge_ySe_{1-y}, where (with some rearrangement) y is given by

$$y = (1+f)x/(3fx+1). \tag{3}$$

We can also express x as a function of y and f as follows:

$$x = y/[1+f(1-3y)]. \tag{4}$$

We note that the limit $f=0$ corresponds to $x=y$, while the limit $f=1$ (all nodal sites are edge-sharing clusters) corresponds to $x=y/(2-3y)$.

The mean coordination of our *simulated* system is given by

$$\langle r\rangle = 2+2x, \tag{5}$$

while the mean coordination of the system *including edge-sharing units* is given by

$$\langle r\rangle' = 2+2y. \tag{6}$$

The widest window produced in our theoretical simulations extends from approximately $\langle r\rangle=2.34$ to $\langle r\rangle=2.4$. These points correspond to $x=0.17$ and $x=0.2$. The maximum shift achievable by this introduction of edge-sharing motifs ($f=1$) would make these equivalent to $y=0.225$ and $y=0.25$, giving $\langle r\rangle'=2.45$ and $\langle r\rangle'=2.5$.

The presence of the edge-sharing tetrahedral motif means that $\langle r\rangle'$ is an *overestimate* of the constraints on the system. The main effect of edge-sharing tetrahedra is to move the center of the window to larger values of $\langle r\rangle'$, accompanied by a slight narrowing of the window. The direction of the shift ($\langle r\rangle<\langle r\rangle'$) helps us bring theory and experiment into closer agreement, with the center of our window being shifted upward in apparent mean coordination by fully 0.1.

It is not only the edge-sharing motif that can be introduced to the system by this approach. Any cluster which is internally rigid and which can accept four links to other Ge sites can be substituted for a single Ge. An example would be a tetrahedron of four Ge atoms (the corners of the tetrahedron) linked internally by six Se atoms (lying on the edges of the tetrahedron); this is an internally rigid unit, with the effect of adding three $GeSe_2$ units to the system. Substitution of such units at a fraction f of Ge sites would give us a composition $y=(1+3f)x/(9fx+1)$, which has an even more dramatic effect on $\langle r\rangle'$ than the edge-sharing unit. Our widest theoretical window ($x=0.17$ to $x=0.2$), on introducing this motif with $f=1$, is shifted to $y=0.269-y=0.286$, giving $\langle r\rangle'=2.54$ and $\langle r\rangle'=2.57$. The window is shifted upward in mean coordination by fully 0.2, while the width decreases by a factor of 2.

We may conclude that the inclusion of internally rigid units such as the edge-sharing motif can account for the center of the experimentally measured window; however, such units cannot account for the wider experimental window, for which some other explanation must be found.

C. Steric interactions

The most important aspect of the physics of rigidity that is absent from our model is jamming due to steric interactions. Our simulated networks are purely topological models, and the decoration and dilution proceed without regard to the steric feasibility of building the network. The development of jammed states in purely steric models has been studied.[28,29] However, there is a fundamental divide between theoretical approaches to steric jamming and to the percolation of rigidity in framework structure. Jamming involves nonholonomic, contact interactions between objects; it requires a model specifying the positions of all objects in the system; it requires consideration of the potential motions of the objects, as jamming occurs when bodies in contact are unable to move apart and relieve the contact; and it is dependent on the boundary conditions of the system, as jamming

requires confinement. The percolation of rigidity, however, involves holonomic constraints describing bonding; it depends on the topology of bonding rather than the exact geometry of the system and does not require exploration of potential motions. Rigidity and stress can occur within a system regardless of whether its boundaries are confined, free, or periodic. It is far from clear what theoretical framework would allow us to investigate rigidity and jamming simultaneously. It is possible that studies on sticky disk systems[30,31] may provide some insight.

Qualitatively, however, we should expect the inclusion of steric interactions to shift both the rigidity and stress transitions to smaller values of $\langle r \rangle$, as we are introducing additional constraints into the system. If the rigidity transition were shifted further than the stress transition, this would offer a mechanism for widening the window.

D. Phase diagram

In Fig. 10, we show the experimentally determined widths of intermediate phases for various glasses, arranged in order of the magnitude of the window and plotted schematically against the structural variability as suggested by the results in this paper by Eq. (2). The x axis is arbitrary, as we lack sufficient information from experiment to establish the scale, but the general scheme is clear. To establish such an absolute scale for the structural variability, it would be necessary to determine the local chemistry and the distribution of lengths of the chains of twofold coordinated atoms from 0 up to 5. This has not been done to date and would be extremely demanding, but could be accomplished by combining NMR, Raman, and measurements of the pair distribution function using isotopes. This presents a major experimental challenge.

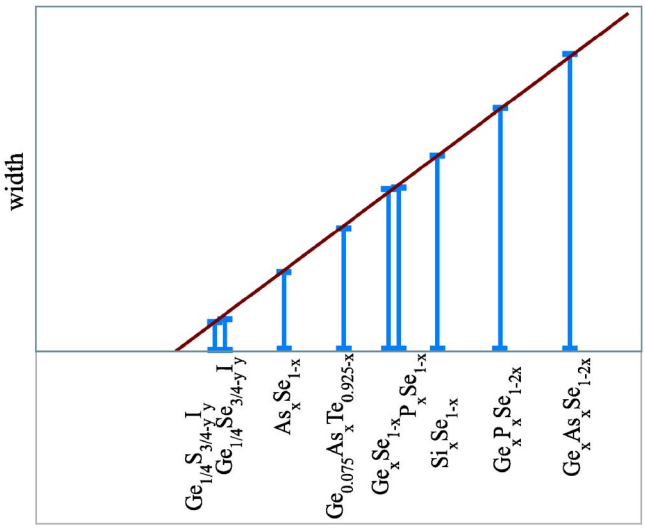

FIG. 10. (Color online) Schematic representation of intermediate phase width in different structures, modified from Wang *et al.* (Ref. 14), where we propose that increasing width of the intermediate phase window indicates increasing structural variability in the system.

ACKNOWLEDGMENTS

We would like to acknowledge ongoing discussions with P. Boolchand, J. Phillips, M. Chubynsky, and N. Mousseau on this subject and support from NSF Grants No. NIRT-0304391 and No. DMR-0425970.

*Present address: Instituto de Ciencias Físicas, Universidad Nacional Autónoma de México, Apartado Postal 48-3, 62251 Cuernavaca, Morelos, Mexico.

[1] M. F. Thorpe, D. J. Jacobs, M. V. Chubynsky, and J. C. Phillips, J. Non-Cryst. Solids **266-269**, 859 (2000).
[2] P. Boolchand, D. G. Georgiev, and B. Goodman, J. Optoelectron. Adv. Mater. **3**, 703 (2001).
[3] P. Boolchand, X. Feng, D. Selvanathan, and W. J. Bresser, in *Rigidity Theory and Applications*, edited by M. F. Thorpe and P. M. Duxbury (Kluwer Academic/Plenum, New York, 1999), p. 279.
[4] M. F. Thorpe, D. J. Jacobs, N. V. Chubynsky, and A. J. Rader, in *Rigidity Theory and Applications*, edited by M. F. Thorpe and P. M. Duxbury (Kluwer Academic/Plenum, New York, 1999), p. 238.
[5] X. W. Feng, W. J. Bresser, M. Zhang, B. Goodman, and P. Boolchand, J. Non-Cryst. Solids **222**, 137 (1997).
[6] J. Gump, I. Finkler, H. Xia, R. Sooryakumar, W. J. Bresser, and P. Boolchand, Phys. Rev. Lett. **92**, 245501 (2004).
[7] D. J. Jacobs, A. J. Rader, L. A. Kuhn, and M. F. Thorpe, Proteins **44**, 150 (2001).
[8] P. Boolchand, X. Feng, and W. J. Bresser, J. Non-Cryst. Solids **293-295**, 348 (2001).
[9] P. Boolchand, G. Lucovsky, J. C. Phillips, and M. F. Thorpe, Philos. Mag. **85**, 3823 (2005).
[10] S. Chakravarty, D. G. Georgiev, P. Boolchand, and M. Micoulaut, J. Phys.: Condens. Matter **17**, L1 (2005).
[11] D. G. Georgiev, P. Boolchand, and K. A. Jackson, Philos. Mag. **83**, 2941 (2003).
[12] U. Vempati and P. Boolchand, J. Phys.: Condens. Matter **16**, S5121 (2004).
[13] Y. Wang, J. Wells, D. G. Georgiev, P. Boolchand, K. Jackson, and M. Micoulaut, Phys. Rev. Lett. **87**, 185503 (2001).
[14] F. Wang, S. Mamedov, P. Boolchand, B. Goodman, and M. Chandrasekhar, Phys. Rev. B **71**, 174201 (2005).
[15] M. V. Chubynsky and M. F. Thorpe, Curr. Opin. Solid State Mater. Sci. **5**, 525 (2001).
[16] J. Barré, A. R. Bishop, T. Lookman, and A. Saxena, Phys. Rev. Lett. **94**, 208701 (2005).
[17] M.-A. Brière, M. V. Chubynsky, and N. Mousseau, Phys. Rev. E **75**, 056108 (2007).
[18] M. V. Chubynsky, M. A. Brière, and N. Mousseau, Phys. Rev. E **74**, 016116 (2006).
[19] M. Micoulaut, Phys. Rev. B **74**, 184208 (2006); M. Micoulaut and J. C. Phillips, J. Non-Cryst. Solids **353**, 1732 (2007).
[20] M. F. Thorpe, D. J. Jacobs, and B. R. Djordjevic, in *Insulating*

and Semiconducting Glasses, Series on Directions in Condensed Matter Physics, edited by P. Boolchand (World Scientific, New York, 2000), Vol. 17, p. 95.
[21] D. J. Jacobs and M. F. Thorpe, Phys. Rev. Lett. **75**, 4051 (1995).
[22] D. J. Jacobs and B. Hendrickson, J. Comput. Phys. **137**, 346 (1997).
[23] B. M. Hespenheide, D. J. Jacobs, and M. F. Thorpe, J. Phys.: Condens. Matter **16**, S5055 (2004).
[24] B. Bureau, J. Troles, M. L. Floch, F. Smektala, and J. Lucas, J. Non-Cryst. Solids **326-327**, 58 (2003).
[25] I. Petri, P. S. Salmon, and H. E. Fischer, Phys. Rev. Lett. **84**, 2413 (2000).
[26] I. Petri and P. S. Salmon, Phys. Chem. Glasses **43C**, 185 (2002).
[27] P. S. Salmon and I. Petri, J. Phys.: Condens. Matter **15**, S1509 (2003).
[28] A. R. Kansal, S. Torquato, and F. H. Stillinger, Phys. Rev. E **66**, 041109 (2002).
[29] C. S. O'Hern, L. E. Silbert, A. J. Liu, and S. R. Nagel, Phys. Rev. E **68**, 011306 (2003).
[30] A. Huerta and G. G. Naumis, Phys. Rev. B **66**, 184204 (2002).
[31] A. Huerta and G. G. Naumis, Phys. Rev. Lett. **90**, 145701 (2003).